Int. J. Heat Mass Transfer. Vol. 20, pp. 945–952. Pergamon Press 1977. Printed in Great Britain

FINITE ELEMENT ANALYSIS OF FREE CONVECTION FLOWS

B. TABARROK and RAN C. LIN
Department of Mechanical Engineering, University of Toronto, Toronto, Canada

(*Received* 3 *August* 1976 *and in revised form* 5 *November* 1976)

Abstract—Two dimensional natural convection problems governed by the continuity, momentum and energy balance equations and simplified through the Boussinesque approximation for buoyancy forces, are studied. By using a stream function the continuity equation is satisfied exactly and the remaining equations are expressed in terms of temperature and vorticity functions. A simple triangular finite element model is then developed and it is employed to analyse two examples, under varying conditions. For the cases where results (experimental and numerical) obtained by other authors are available a comparison is made. This comparison exhibits good agreement.

NOMENCLATURE

A_e,	area of an element;
d,	significant length scale of the domain;
g,	gravitational constant;
Gr,	Grashof number, $g\beta(T_h-T_c)d^3/\nu^2$;
$\bar{h}$,	average heat-transfer coefficient;
$\mathbf{i}, \mathbf{j}$,	unit vectors in x and y directions;
k,	thermal conductivity;
l,	cavity height;
$\mathbf{n}, \mathbf{t}$,	outward and tangential unit vectors;
Nu,	Nusselt number $\bar{h}d/k$;
n_x, n_y,	direction cosines;
$P, (p)$,	dimensional (dimensionless) fluid pressure;
Pr,	Prandtl number, ν/α;
Ra,	Rayleigh number, $g\beta(T_h-T_c)d^3/\nu\alpha$;
T,	local temperature;
T_h, T_c, T_0,	temperature of hot, cold walls of cavity and average temperature;
$u, v, (U, V)$,	dimensional (dimensionless) velocity components in x, y direction;
u_n, u_t,	dimensionless velocity components in normal and tangential direction;
$x, y, (X, Y)$,	dimensional (dimensionless) coordinates;
$[N(x, y)]$,	row matrix for element interpolating function;
$\{q\}, \{q\}^t$,	column matrix and its transpose for element nodal values;
$[K_\theta^*], [K_\omega^*], [K_\psi^*]$,	global system matrices for temperature, vorticity and stream functions;
$\{q_\theta^*\}, \{q_\omega^*\}, \{q_\psi^*\}$,	global vectors for temperature, vorticity and stream function nodal values;
$\{Q_\theta^*\}, \{Q_\omega^*\}, \{Q_\psi^*\}$,	global load vectors for temperature, vorticity, and stream functions.

Greek letters

α,	fluid thermal diffusivity;
β,	coefficient of thermal expansion;
γ,	aspect ratio of rectangular cavity, l/d;
θ,	dimensionless temperature, $(T-T_0)/(T_h-T_0)$;
ν,	fluid kinematic viscosity;
ρ, ρ_0,	fluid density, fluid density corresponding to average temperature;
ψ,	dimensionless stream function;
ω,	dimensionless vorticity, $(\partial V/\partial X - \partial U/\partial Y)$.

INTRODUCTION

NATURAL convection flows induced by buoyancy forces arise in many spheres of application. As examples of current interest we may cite the problem of heat effluent dispersion in estuaries and that of cooling fluids in channels surrounding a nuclear reactor core. Such flows have been the subject of experimental and theoretical investigations over the last two decades. A brief account of historical developments of the subject along with explanation of assumptions inherent in the governing equations of the problem are given by De Vahl Davis [1]. Essentially the governing equations are statements of conservation of mass, momentum and energy. To obtain a solution for these coupled non-linear equations, one must resort to a numerical method of solution. Amongst such methods the finite difference procedures have been most popular. These procedures are particularly convenient for rectangular domains over which a uniform rectangular mesh can be used.

In recent years notable progress has been made in the development of finite element procedures for flow problems [2, 3]. In these procedures the generation of discrete equations for a non-uniform mesh, over a domain with an irregular boundary is relatively easy and herein lies the main advantage of the finite element procedure over the finite difference approach.

The aim of the present investigation is two fold. First a finite element model is developed for the solution of the two dimensional natural convection problems. Then by the way of illustrative examples some simple cases of different configuration are analysed and where results obtained by other procedures are available, a comparison is made.

FORMULATION OF THE PROBLEM

We consider the two-dimensional steady-state analysis of an incompressible fluid driven by buoyancy forces. It is assumed that these forces can be sufficiently accurately described by the Boussinesque approximation. In this approximation the changes in density are expressed directly in terms of changes in temperature only and the resulting buoyancy forces are then introduced into the equilibrium equations in the form of body forces. However, the density changes are ignored in the inertia terms of the equilibrium equations and the continuity equation. It is further assumed that the dissipation due to viscous forces in the equilibrium equations, does not contribute significantly to the energy transport equation.

Under these assumptions the conservation of mass, momentum and energy may be expressed as

$$\frac{\partial u}{\partial x}+\frac{\partial v}{\partial y}=0 \tag{1}$$

$$u\frac{\partial u}{\partial x}+v\frac{\partial u}{\partial y}=-\frac{1}{\rho_0}\frac{\partial p}{\partial x}+\frac{g(\rho-\rho_0)}{\rho_0}+\nu\nabla^2 u \tag{2}$$

$$u\frac{\partial v}{\partial x}+v\frac{\partial v}{\partial y}=-\frac{1}{\rho_0}\frac{\partial p}{\partial y}+\nu\nabla^2 v \tag{3}$$

$$u\frac{\partial T}{\partial x}+v\frac{\partial T}{\partial y}=\alpha\nabla^2 T \tag{4}$$

where various symbols have their conventional meanings and the subscript 0 denotes a reference temperature which we take as the mean of the hot and cold temperatures, see Fig. 1. Now the buoyancy force which acts in the direction of x axis, may be expressed in terms of temperature changes through the Boussinesque approximation

$$\frac{\mathrm{d}\rho}{\rho_0}=-\beta\,\mathrm{d}T \quad \beta\text{, thermal expansion coefficient}$$

and hence

$$\frac{\rho-\rho_0}{\rho_0}=-\beta(T-T_0). \tag{5}$$

Substitution from equation (5) into equation (2) will close the system equations (2)–(4) in terms of the four

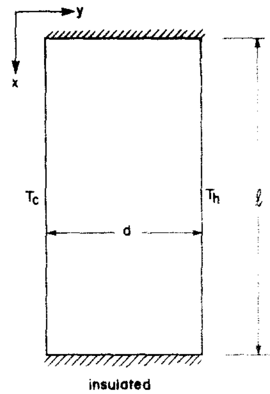

FIG. 1. The coordinate system.

unknowns u, v, p and T. It is convenient to cast the system equations into non-dimensional form. To this end we introduce the following dimensionless variables.

$$X=x/d,\quad Y=y/d,\quad \theta=\frac{T-T_0}{T_h-T_0},$$
$$U=ud/\nu,\quad V=vd/\nu,\quad P=pd^2/\rho_0\nu^2.$$

To obtain approximate solutions for the four system equations one may proceed in a number of different ways. Specifically in the case of finite element analysis, three methods have been developed. In the first the discretised equations are obtained directly in terms of U, V, P and θ. This procedure has been employed by a number of authors for the analysis of viscous flow problems, i.e. only the momentum and the continuity equations are considered. As examples of this procedure we may cite the works of Hood and Taylor [3], Kawahara *et al.* [3] and Oden and Welford [4]. More recently the same procedure has been employed for convection problems by Kawahara *et al.* [5], Zienkiewicz *et al.* [6], and Gartling and Nickel [7]. A second alternative, which we follow, satisfies the continuity equation identically by introduction of the stream function ψ, defined as

$$U=\frac{\partial\psi}{\partial Y},\qquad V=-\frac{\partial\psi}{\partial X}. \tag{6}$$

Further, the pressure is eliminated from the momentum equations by appropriate differentiations and subtraction. The introduction of the vorticity function ω, defined as

$$\omega=\frac{\partial V}{\partial X}-\frac{\partial U}{\partial Y} \tag{7}$$

then allows one to describe the flow problem, in the absence of energy balance equation, in terms of the two variables ψ and ω. This, the so-called vorticity-stream function formulation has also been employed by a number of authors for the solution of the two-dimensional momentum and continuity equations. As examples we cite the works of Baker [8, 9], Cheng [10], Smith and Brebbia [11], Tong [12], and Bratanow *et al.* [13].

A third alternative requires the elimination of the vorticity function through equations (6) and (7). This procedure which leads to a fourth order equation in terms of ψ, has been used by Olson [14] and Kawahara and Okamoto [15] for analysis of flow problems and by Young *et al.* for analysis of convection problems [16].

In regard to advantages of one formulation over another the following comments can be made. Evidently the number of variables in the last procedure, is least and this may be considered as an advantage for this formulation. However, the reduction in the number of variables is gained at the expense of admitting higher order derivatives in the system equation(s). The implications of these higher derivatives is two fold. First, the continuity of the variable(s) from one element to the next, becomes stringent and difficult to meet [17]. Second, while the accuracy of computed values of ψ may be acceptable, those of the velocities will generally be inferior as a consequence of differentiations of an approximate field of ψ. These features of the stream function formulation make the use of high degree polynomials, as shape functions, mandatory [14]. The stream function–vorticity formulation also suffers from the loss of accuracy that results when the velocities are derived from the stream function. However, in this formulation the requirements of continuity of ψ and ω from one element to the next do not present particular problems.

The main drawback of the direct formulation for flow problems is the fact that the continuity equation is in effect, used as a constraint and is only approximately satisfied. This raises the question of relative accuracy required for the momentum equations versus that of the continuity equation. Further the manner in which the continuity equation is incorporated into the discretised equations gives rise to some zero elements along the diagonals of one system matrix and prevents one from using some standard solver routines.

On balance, the vorticity–stream function formulation appears to us to be the most suitable for the problem at hand and hence its adoption here.

It can be readily shown that in terms of the non-dimensional variables the energy balance, and the momentum equations appear as

$$\frac{\partial\psi}{\partial Y}\frac{\partial\theta}{\partial X}-\frac{\partial\psi}{\partial X}\frac{\partial\theta}{\partial Y}=\frac{1}{Pr}\nabla^2\theta \quad (8)$$

$$\frac{\partial\psi}{\partial Y}\frac{\partial\omega}{\partial X}-\frac{\partial\psi}{\partial X}\frac{\partial\omega}{\partial Y}=\frac{Gr}{2}\frac{\partial\theta}{\partial Y}+\nabla^2\omega \quad (9)$$

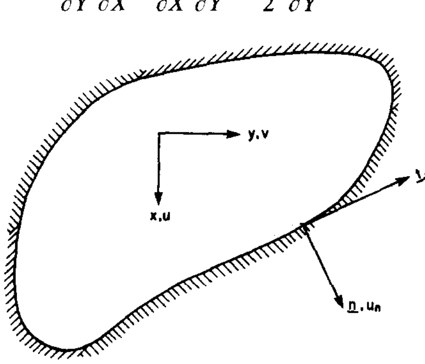

FIG. 2. Domain and boundary variables.

where $Gr = g\beta(T_h - T_c)d^3/\nu^2$ is the Grashof number and $Pr = \nu/\alpha$, the Prandtl number.

Further, from equations (6) and (7) we have

$$\nabla^2\psi = -\omega. \quad (10)$$

Equations (8)–(10) constitute the governing equations of the problem.

Next consider the associated boundary conditions. For generality consider a curved boundary with an outward normal vector $\mathbf{n}(=\mathbf{i}n_x+\mathbf{j}n_y)$ as shown in Fig. 2. Then for the temperature boundary conditions we have; either θ is prescribed or

$$\frac{\partial\theta}{\partial\mathbf{n}} = 0. \quad (11)$$

For the velocity boundary conditions we first transform the velocities U and V to the boundary velocities U_n and U_t as shown in Fig. 2. Thus

$$U_n = n_x U + n_y V \quad (12)$$

$$U_t = -n_y U + n_x V. \quad (13)$$

Now for confined flows U_n and U_t must vanish. This implies that along a solid boundary

$$\frac{\partial\psi}{\partial\mathbf{t}} = 0 \quad \frac{\partial\psi}{\partial\mathbf{n}} = 0. \quad (14)$$

Also from the definition of the stream function it is evident that the value of ψ is arbitrary to within a constant. As such ψ can be equated to zero at least at one point of a simply connected domain. If this point is taken on a solid boundary then from the first of equation (14) it follows that ψ must be zero along the entire length of the solid boundary.

Equations (11) and (14) constitute the essential boundary conditions of the problem. However, solution of equation (9) requires appropriate boundary conditions for the vorticity ω. These boundary conditions can be deduced from equation (8). Thus using the axes (**n**, **t**) on the boundary and recalling that $\psi \equiv 0$ along a solid wall, we have in this case;

$$\omega = -\frac{\partial^2\psi}{\partial\mathbf{n}^2}. \quad (15)$$

SOLUTION STRATEGY AND FINITE ELEMENT EQUATIONS

System equations (8)–(10) form a set of quasilinear elliptic equations. As such the solutions for ψ, ω and θ will be continuous in the domain. The equations may be solved in the following iterative procedure.

Initially the stream function is assumed as zero everywhere and equation (9) is then solved as a linear equation for θ. This solution describes the temperature distribution for the pure conduction case. This temperature distribution and the associated stream function field are then substituted into equation (9) from which a distribution for vorticity is obtained. Finally the obtained vorticity distribution is used in equation (10) and an improved distribution for ψ is determined. The cycle of iteration is then repeated until the values of ω for two consecutive calculations are within certain prescribed limits.

To develop the discrete system equations consider a triangular element over which we approximate the stream function, temperature and vorticity by polynomials in X and Y. Since the three differential equations are of equal order, there is no need to use polynomials of different degrees for the three unknowns.

To outline the method of discretisation of differential equations (8)–(10) we represent all three in the following form

$$\frac{\partial^2 \phi}{\partial X^2}+\frac{\partial^2 \phi}{\partial Y^2}+\bar{S}(X, Y)=0 \tag{16}$$

where ϕ represents the stream function, temperature and vorticity in turn but $\bar{S}(X, Y)$ takes different forms in each case. If we consider $\bar{S}(X, Y)$ to be a prescribed function in each case, then equation (16) will be the Euler–Lagrange equation of the following functional

$$I=\int_A\left\{\frac{1}{2}\left[\left(\frac{\partial \phi}{\partial X}\right)^2+\left(\frac{\partial \phi}{\partial Y}\right)^2\right]-\bar{S}(X, Y)\phi\right\}\mathrm{d}A. \tag{17}$$

The bar over the function $\bar{S}$ indicates that this function is prescribed and does not participate in the process of variation. It is a simple matter to show that extremisation of I yields equation (16) as well as the following associated boundary condition

$$\frac{\partial \phi}{\partial \mathbf{n}}\,\delta\phi=0. \tag{18}$$

Equation (18) admits two types of boundary conditions —the so-called essential and natural types. For equation (18) to be satisfied either ϕ must be prescribed or $\partial\phi/\partial\mathbf{n}$ must vanish naturally through the process of extremisation. When ϕ stands for temperature the first type of boundary condition refers to a given temperature distribution along a boundary while the second type describes an insulated boundary across which heat flux must vanish. When ϕ stands for the stream function the appropriate boundary condition, on a solid wall, is of the essential type and as mentioned earlier the value of ψ is prescribed as zero along the boundary. Hence

$$\frac{\partial \psi}{\partial t}=U_n=0. \tag{19}$$

It is worth noting that the no-slip boundary condition namely $U_t=0$, is not imposed by prescribing ψ along the boundary. We shall see shortly how this boundary condition is imposed.

When ϕ stands for vorticity, again the required boundary condition for a solid wall is of the essential type. Thus we prescribe the vorticity along the boundary. The required value, as mentioned earlier, is obtained from the calculated values of ψ via equation (15). To this end we expand ψ in a Taylor series, at the solid wall, and obtain

$$\psi_i=\psi_w+\left.\frac{\partial \psi}{\partial \mathbf{n}}\right|_w(\Delta n)+\tfrac{1}{2}\left.\frac{\partial^2 \psi}{\partial \mathbf{n}^2}\right|_w(\Delta n)^2+\ldots \tag{20}$$

where ψ_i is the value of the stream function a small distance (Δn) along the normal and inside the domain and the subscript w stands for wall. Now we let $\partial\psi/\partial\mathbf{n}/_w=0$ and thereby we impose the no-slip boundary condition. Further, since $\psi_w=0$ we have from equations (15) and (20) the following approximation for the prescribed value of ω along the boundary

$$\omega=-\frac{2\psi_i}{(\Delta n)^2}. \tag{21}$$

Now returning to equation (17) we note that, for the functional I to be integrable, ϕ must be continuous everywhere in the domain. Hence in the finite element discretisation the competing functions must be continuous within and across elemental boundaries. The simplest way of satisfying this requirement is to use linear interpolation (or shape) functions over an element. Thus we let

$$\phi(X, Y)=[N(X, Y)]\{q\} \tag{22}$$

where $[N(X, Y)]$ is a 1×3 row matrix of interpolation functions and $\{q\}$ denotes the value of ϕ at 3 vertices of a triangular element. The details of derivation of $[N(X, Y)]$ can be found in any text on the finite element method, e.g. Zienkiewicz [17]. Substituting from equation (22) into equation (17) we obtain the following discrete form of I

$$I=\sum_{e=1}^{M}\int_{A_e}\left\{\tfrac{1}{2}\{q\}^t\left(\left\{\frac{\partial N}{\partial X}\right\}\left[\frac{\partial N}{\partial X}\right]+\left\{\frac{\partial N}{\partial Y}\right\}\left[\frac{\partial N}{\partial Y}\right]\right)\{q\}-\bar{S}(X, Y)[N]\{q\}\right\}\mathrm{d}A \tag{23}$$

where the integration is over each element and the summation is over the number of elements. In our case since the interpolation functions are simple in nature and the elements are straight sided, the integration in equation (23) can be carried out in close form. In any event the result of integrations in equation (23) will yield discrete equations of the following form

$$I=\sum_{e=1}^{M}\tfrac{1}{2}\{q\}^t([K_e]\{q\}-\{Q_e\}) \tag{24}$$

where the elemental matrices $[K_e]$ and $\{Q_e\}$ are obtained from

$$[K_e]=\int_{A_e}\left[\frac{\partial N}{\partial X}\;\frac{\partial N}{\partial Y}\right]\begin{bmatrix}\dfrac{\partial N}{\partial X}\\[2mm]\dfrac{\partial N}{\partial Y}\end{bmatrix}\mathrm{d}A \tag{25}$$

and

$$\{Q_e\}=\int_{A_e}[N]\bar{S}(X, Y)\,\mathrm{d}A. \tag{26}$$

Finally, all the elemental nodal variables $\{q\}$ are related to a set of independent global nodal variables $\{q^*\}$ and thereby the continuity requirement for ϕ, from one element to the next, is imposed. The functional I may then be expressed in terms of the global matrices as

$$I=\tfrac{1}{2}\{q^*\}^t[K^*]\{q^*\}-\{q^*\}^t\{Q^*\} \tag{27}$$

where the global matrices $[K^*]$ and $\{Q^*\}$ are obtained from those of the elements (see [17]). Extremisation

Table 1. Summary of the test runs for example 1

Run	γ	*Pr*	*Gr*	*Nu*	
1	1	0.733	10^3	1.073	(Uniform mesh size)
2	1	0.733	5×10^3	1.653	(Uniform mesh size)
3	1	0.733	10^4	2.108	(Uniform mesh size)
4	1	0.733	2×10^4	2.695	(Uniform mesh size)
5	3	0.733	2×10^4	2.568	(Uniform mesh size)
6	0.5	0.733	2×10^4	1.630	(Uniform mesh size)
7	0.2	0.733	2×10^4	1.07	(Non-uniform mesh size)
8	0.2	6.983	2×10^4	1.14	(Uniform mesh size)
9	0.2	6.983	2×10^4	1.59	(Non-uniform mesh size)

Table 2. A comparison with previous results for example 1

Authors	Aspect ratio γ	*Ra*	*Nu*	
Present	1	1.47×10^4	2.695	
Catton *et al.*	1	1.47×10^4	2.71	Galerkin method
Cormack *et al.*	1	1.47×10^4	2.64	21×21 F.D.
Wilkes *et al.*	1	1.47×10^4	2.874	11×11 F.D.
Wilkes *et al.*	1	1.47×10^4	2.516	21×21 F.D.
Ozoe *et al.*	1	1.47×10^4	2.75	
Present	3	1.47×10^4	2.568	
Wilkes *et al.*	3	1.47×10^4	2.825	11×11 F.D.
Ozoe *et al.*	3	1.47×10^4	2.71	
Present	0.2	1.47×10^4	1.07	
Catton *et al.*	0.2	1.47×10^4	1.05	Galerkin method
Present	0.2	1.4×10^5	1.14	Uniform mesh size
Present	0.2	1.4×10^5	1.59	Non-uniform mesh size
Catton *et al.*	0.2	1.4×10^5	1.17	Galerkin method

of I with respect to $\{q^*\}$ yields the discrete equations for the system as

$$\{K^*]\{q^*\} = \{Q^*\}. \tag{28}$$

In the present formulation we have three sets of discrete equations associated with equations (8)–(10).

$$[K_\theta^*]\{q_\theta^*\} = \{Q_\theta^*(\psi)\} \tag{29}$$

$$[K_\omega^*]\{q_\omega^*\} = \{Q_\omega^*(\psi,\theta)\} \tag{30}$$

$$[K_\psi^*]\{q_\psi^*\} = \{Q_\psi^*(\omega)\}. \tag{31}$$

These equations are coupled, in a non-linear manner, through the RHS column vectors as indicated. A comparison with equations (8)–(10) also reveals that the parameter *Pr* enters the calculation via $[K_\theta^*]$ while *Gr* is accounted for in $\{Q_\omega^*\}$. The algebraic equations (29)–(31) are then solved in an iterative scheme as described earlier.

ILLUSTRATIVE EXAMPLES

The element developed here has been used to analyse a number of examples. For the sake of economy in space we report the results of two examples here. In [18], other examples, with extensive details of results, are described.

In the first example a rectangular cavity is considered. The non-dimensional temperature θ, is taken as -1 along the wall $y = 0$ and $+1$ along the opposite wall. The remaining two walls are considered as insulated (see Fig. 1). Nine different cases for some variations of aspect ratio γ, Grashof number *Gr* and Prandtl number *Pr*, have been analysed and the results are shown in Table 1. In all cases 200 triangular elements resulting in 121 nodes, were used in the computations. In most cases a uniform mesh was adopted but in two cases non uniform meshes were tested. For obtaining the boundary values of ω from equation (21) the values of ψ at the nodes closest to the boundary were used and (Δ_n) was computed for such nodes. The average value of Nusselt number *Nu*, given in Table 1, was calculated from

$$Nu = \frac{1}{2\gamma}\int_0^\gamma \frac{\partial\theta}{\partial Y}\,\mathrm{d}X, \quad \gamma = \text{aspect ratio}.$$

The case of the rectangular cavity with differentially heated walls has been analysed by other authors using other numerical procedures. Some of the published results are given in Table 2 along with corresponding results obtained by the present finite element formulation. The parameter *Ra*, appearing in Table 2, is the Rayleigh number given by the product of *Gr* and *Pr*.

According to the work of Catton *et al.* [19] the maximum value of *Nu*, at a given value of Rayleigh's number, occurs at aspect ratio $\gamma = 1$. This feature is borne out by the results given in Table 2. For this particular value of aspect ratio the results of present formulation are generally in good agreement with those obtained by other authors. However, at aspect ratio $\gamma = 3$ the finite element results appear lower than those reported by Wilkes *et al.* [20] and Ozoe *et al.* [21].

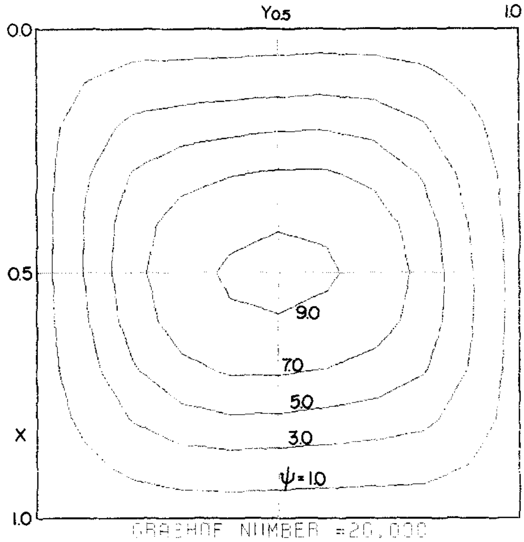

FIG. 3. Iso-stream lines for $\gamma = 1$ and $Pr = 0.733$.

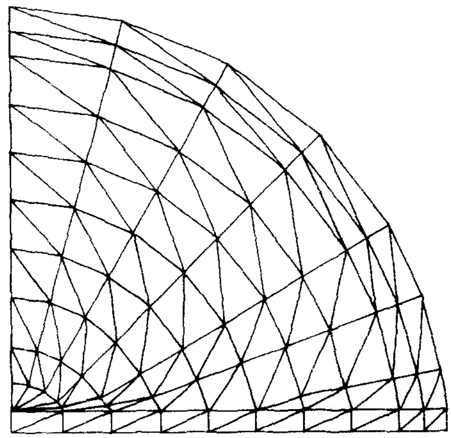

FIG. 6. Element discretisation of quadrant of circular region.

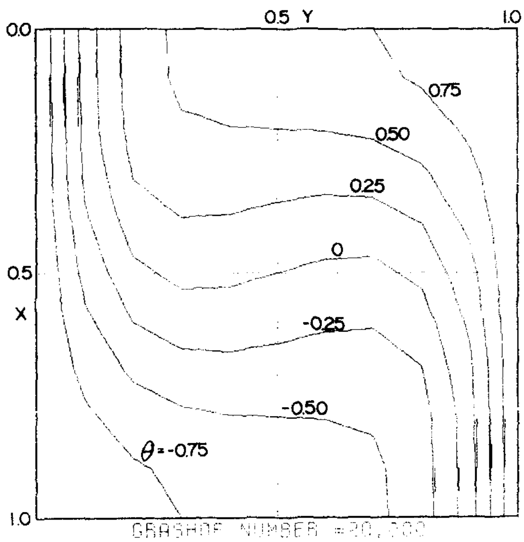

FIG. 4. Iso-thermals for $\gamma = 1$ and $Pr = 0.733$.

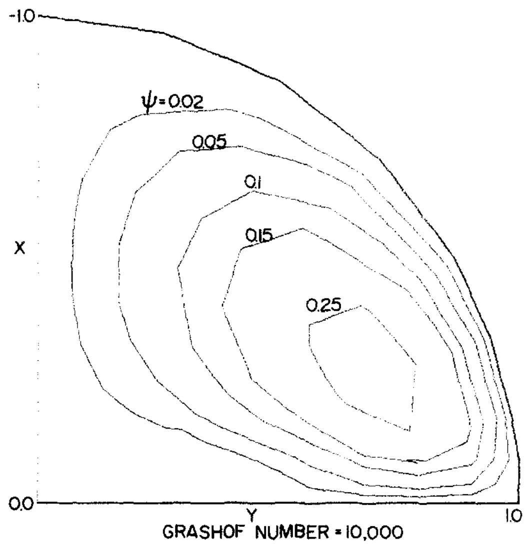

FIG. 7. Iso-stream lines for $Pr = 7.00$.

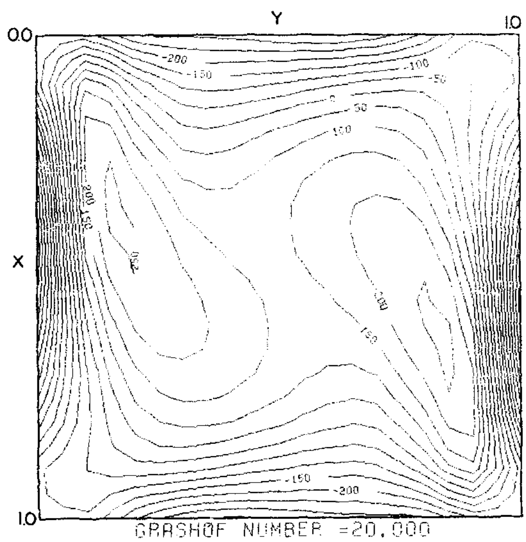

FIG. 5. Iso-vorticity lines for $\gamma = 1$ and $Pr = 0.733$.

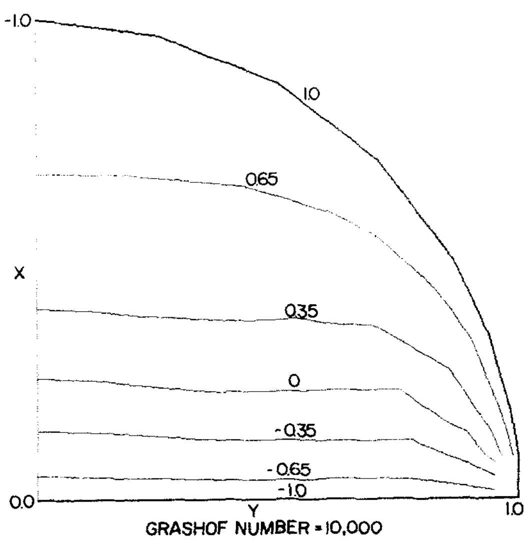

FIG. 8. Iso-thermal lines for $Pr = 7.00$.

However, Ozoe and his co-workers found that generally their experimental results were lower than their theoretically predicted values. Unfortunately no comparable experimental results were given for aspect ratio $\gamma = 3$, in [21]. Nevertheless it is expected that the present finite element results are more accurate than those quoted in [20, 21]. As to the case of aspect ratio $\gamma = 0.2$, the present results are again in good agreement with those obtained by other authors.

In Figs. 3–5 computer plots of iso-streamlines, isothermal lines and iso-vorticity lines are depicted for the case of aspect ratio $\gamma = 1$ and Grashof number 20000. Comparison of these plots with the corresponding ones given in [20], shows good agreement.

As a second example a semi-circular cavity was considered. On the curved boundary it was assumed that $\theta = +1$ while on the straight boundary θ was prescribed equal to -1. Due to the symmetry of the domain and its boundary conditions, only half the semi-circular cavity was analysed. Figure 6 shows the element discretisation of the domain while Figs. 7 and 8 depict computer plots for iso-stream and iso-thermal lines for the case of $Pr = 7.00$ and $Gr = 10\,000$.

CONCLUSIONS

A simple finite element model has been developed for the steady state analysis of free convection problems. Results have been computed for several examples with varying aspect ratios, boundary conditions and Rayleigh numbers. Where there exist corresponding results obtained experimentally or by other numerical or analytical methods, a comparison is made. In general very good agreement has been found in this comparison.

Acknowledgement—The investigation presented here has been partially supported by Grant No. A3818 of National Research Council of Canada.

REFERENCES

1. G. De Vahl Davis, Laminar natural convection in an enclosed rectangular cavity, *Int. J. Heat Mass Transfer* **11**, 1675–1693 (1968).
2. C. Brebbia and J. J. Connor (editors), *Proceedings of the Symposium on Numerical Methods in Fluid Dynamics*. Pentech Press, London (1974).
3. J. T. Oden, O. C. Zienkiewicz, R. H. Gallagher and C. Taylor (editors), *Proceedings of the International Symposium on Finite Element Methods in Flow Problems, Swansea, U.K.* University of Alabama Press, Huntsville (1974).
4. J. T. Oden and L. C. Welford, Analysis of flow of viscous fluids by the finite element method, *AIAA Jl* **10**(12), 1590–1599 (1972).
5. M. Kawahara, N. Yoshimura, K. Nakagawa and H. Ohsaka, Steady and unsteady finite element analysis of incompressible viscous fluid, *Int. J. Num. Methods Engng* **10**, 437–456 (1976).
6. O. Zienkiewicz, R. Gallagher and P. Hood, Newtonian and non-Newtonian viscous incompressible flow, temperature induced flow, Proc. Conf. on Math. of Finite Elements and Applications, Brunel University (April 1974).
7. K. Gartling and R. Nickell, Free and forced convective-diffusion solutions by finite element methods, Proc. of 2nd Int. Conf. on Finite Element Methods in Flow Problems, St. Margherita, Italy (June 1976).
8. A. J. Baker, Finite element solution algorithm for viscous incompressible fluid dynamic, *Int. J. Num. Methods Engng* **6**, 89–101 (1973).
9. A. J. Baker, A highly-stable explicit integration technique for computational continuum mechanics, in *Proceedings of Conference on Numerical Methods in Fluid Dynamics*, pp. 99–120. Pentech Press, London (1974).
10. R. T. Cheng, Numerical solution of the Navier–Stokes equations by the finite element method, *Physics Fluids* **15**, 2098–2105 (1972).
11. S. L. Smith and C. A. Brebbia, Finite element solution of Navier–Stokes equations for transient two-dimensional incompressible flow, *J. Comput. Phys.* **17**(3), 235–245 (1975).
12. P. Tong, The finite element method for fluid flow, in *Proceedings of the Conference on Recent Advances in Matrix Methods of Structural Analysis and Design*, pp. 787–808. University of Alabama Press, Huntsville (1971).
13. T. Bratanow, A. Ecer and M. Kobiske, Finite element analysis of unsteady incompressible flow around an oscillating obstacle of arbitrary shape, *AIAA Jl* **11**(11), 1471–1477 (1973).
14. M. D. Olson, Formulation of a variational principle-finite element method for viscous flow, in *Proceedings of the Conference on Variational Methods in Engineering*, Vol. 1. Southampton University Press, Southampton (1973).
15. M. Kawahara and T. Okamoto, Finite element analysis of steady flow of viscous fluid using stream function, *Proc. J.S.C.E.* No. 247 (1976).
16. D. L. Young, J. A. Ligget and R. H. Gallagher, Steady stratified circulation in a cavity, *J. Engng Mech. Div. Am. Soc. Civ. Engrs* **102**(EM1) (1976).
17. O. C. Zienkiewicz, *The Finite Element Method in Engineering Science*. McGraw-Hill, New York (1971).
18. B. Tabarrok and R. C. Lin, Finite element analysis of free convection flows, Dept. of Mechanical Engineering Technical Publication Series, UTME-TP 7602, University of Toronto, Canada (1976).
19. I. Catton, P. S. Ayyaswamy and R. M. Clever, Natural convection flow in a finite rectangular slot arbitrarily oriented with respect to the gravity vector, *Int. J. Heat Mass Transfer* **17**, 173–184 (1974).
20. J. O. Wilkes and S. W. Churchill, The finite-difference computation of natural convection in a rectangular enclosure, *A.I.Ch.E. Jl* **12**, 161–166 (1966).
21. H. Ozoe, H. Sayama and S. W. Churchill, Natural convection in an inclined rectangular channel at various aspect ratios and angles—experimental measurements, *Int. J. Heat Mass Transfer* **18**, 1425–1431 (1975).

ANALYSE PAR ELEMENTS FINIS DES ECOULEMENTS DE CONVECTION NATURELLE

Résumé—On étudie les problèmes de convection naturelle bidimensionnelle, gouvernés par les équations de continuité, de quantité de mouvement et d'énergie et simplifiés par l'approximation de Boussinesq pour les forces d'Archimède. Par l'utilisation d'une fonction de courant, l'équation de continuité est satisfaite exactement et les équations restantes sont exprimées en termes de fonctions de température et de vorticité. On développe un modèle simple à élément fini triangulaire et on l'utilise pour analyser deux exemples sous des conditions variées. On fait une comparaison avec les résultats (expérimentaux et numériques) obtenus par d'autres auteurs. Cette comparaison montre un bon accord.

DIE UNTERSUCHUNG FREIER KONVEKTIONSSTRÖMUNGEN MIT HILFE FINITER ELEMENTE

Zusammenfassung— Die durch Kontinuitäts-, Impuls- und Energiegleichung bestimmte zweidimensionale freie Konvektion wird untersucht, wobei die Boussinesque-Näherung für die Auftriebskräfte angesetzt wurde. Die Kontinuitätsgleichung wird mit Hilfe einer Stromfunktion exakt gelöst; die verbleibenden Gleichungen werden mit Temperatur- und Wirbelfunktionen ausgedrückt. Es wird ein einfaches Modell mit dreieckigen finiten Elementen entwickelt und auf zwei Beispiele unter variablen Bedingungen angewandt. Für die Fälle, für die experimentelle oder numerische Ergebnisse anderer Autoren vorliegen, wird ein Vergleich durchgeführt, wobei sich eine gute Übereinstimmung ergibt.

АНАЛИЗ СВОБОДНОКОНВЕКТИВНЫХ ТЕЧЕНИЙ МЕТОДОМ КОНЕЧНЫХ ЭЛЕМЕНТОВ

Аннотация — Исследуются двумерные задачи по свободной конвекции, описываемые уравнениями неразрывности, количества движения и энергии, которые упрощены благодаря введению приближения Буссинеска для подъемных сил. В результате использования функции тока уравнение неразрывности удовлетворяется точно, а оставшиеся уравнения выражаются через функции температуры и завихренности. Далее, разработана простая конечноэлементная модель треугольного типа, с помощью которой анализируются два примера при изменяющихся условиях. Полученные результаты хорошо согласуются с имеющимися экспериментальными данными.